Journal of Environmental Biology
p-ISSN: 0254-8704 • e-ISSN: 2394-0379 • CODEN: JEBIDP

JEB®

Original Research Paper
Volume 47 Issue 2 March 2026 pp. 219-229
DOI: http://doi.org/10.22438/jeb/47/2/MRN-5675

J. Environ. Biol., 2026

Journal website : www.jeb.co.in ★ E-mail : editor@jeb.co.in

Effective and sustainable fluoride removal from aqueous solutions using chemically functionalized biochar and pellet based column system

M.M. Girkar[1,2], S.P. Shukla[1]*, S. Kumar[1], K. Kumar[1], V.S. Bharti[1], G.R. Bhuvaneshwari[3], S.S. Gangan[4], S.W. Belsare[2] and S.N. Kunjir[5]

[1]*Aquatic Environment & Health Management Division, ICAR-Central Institute of Fisheries Education, Mumbai- 400 061, India*
[2]*Department of Aquatic Environment Management, Maharashtra Animal and Fishery Sciences University, Nagpur, 440 001, India*
[3]*Mariculture Division, ICAR-CMFRI, Vizhinjam Regional Centre, Thiruvananthapuram-695 001, India*
[4]*Department of Fisheries Resource Management, Taraporevala Marine Biological Research Station, Mumbai- 400 051, India*
[5]*Department of Fisheries Extension, Economics & Statistics, Maharashtra Animal and Fishery Sciences University, Nagpur-440 001, India*

Received: 25 January 2025 **Revised:** 23 April 2025 **Accepted:** 15 October 2025

***Corresponding Author Email:** spshukla@cife.edu.in ***ORCiD:** https://orcid.org/0000-0002-8908-8701

Abstract

Aim: This study aims to assess the fluoride-removal performance of a unique column-bed prototype designed for water treatment.

Methodology: In batch and column study, the efficacy of the adsorbent chemically functionalized sugarcane bagasse biochar (FSB) in fluoride removal (water spiked with sodium fluoride) was examined under diverse conditions. The adsorption process was analyzed by the Langmuir and Freundlich isotherms, while the kinetics was examined using the pseudo-first and pseudo-second-order models. The column bed, prepared from low-cost pellets of Plaster of Paris, bagasse filaments, and FSB, was tested under varying flow rates, bed heights, and electric charges.

Results: Optimal fluoride removal (78.6%) was achieved at 60 min contact, 150 mg 100 ml^{-1} adsorbent, 5.0 mg l^{-1} fluoride, 120 rpm agitation, and pH 5.0. Adsorption followed the Freundlich model and pseudo-second-order kinetics, indicating chemisorption, while column studies showed improved removal with increased bed height and lower flow velocity.

Interpretation: This study introduces a novel column-bed reactor design for fluoride removal, employing pelleted FSB packing material as a unique approach to enhance efficiency.

Key words: Adsorption, Chemically functionalized biochar, Column study, Fluoride, Sugarcane bagasse

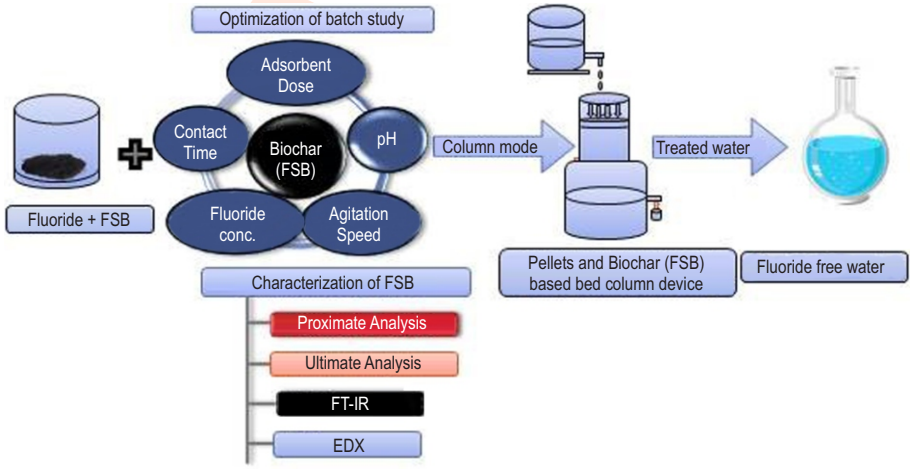

How to cite: Girkar, M.M., S.P. Shukla, S. Kumar, K. Kumar, V.S. Bharti, G.R. Bhuvaneshwari, S.S. Gangan, S.W. Belsare and S.N. Kunjir: Effective and sustainable fluoride removal from aqueous solutions using chemically functionalized biochar and pellet based column system. *J. Environ. Biol.*, **47**, 219-229 (2026).

Introduction

Fluoride is among the most abundant elements on earth, present in nearly all groundwater globally. Groundwater is the primary source of drinking water for a substantial segment of the global population (Chamanehpour *et al.,* 2020). Groundwater fluoride pollution constitutes a significant problem impacting millions of individuals worldwide (Alhendal *et al.,* 2020; Derakhshani *et al.,* 2020). Currently, the utilization of freshwater is increasing at remarkable speed, driven by rapid industrial growth, rise in global population, the expansion of mechanized agriculture, and rapid urbanization (Fito and Alemu, 2019; Fito *et al.,* 2017). Fluorite, biotite, topaz, fluorapatite, cryolite, hornblende, and muscovite are examples of rocks with fluoride-rich minerals. When these minerals come into contact with water, they produce fluoride (Rizzu *et al.,* 2021). The concentration of fluoride in groundwater is influenced by various factors, including the physical and chemical characteristics of the aquifer (Raj and Shaji, 2017), the degree of rock weathering, the water depth within the aquifer (Raju *et al.,* 2012), soil and rock acidity and porosity, interactions among chemical elements, regional temperature (Singaraja *et al.,* 2014), mineral composition of rocks, and the geochemistry of groundwater (Patel *et al.,* 2018).

Fluoride concentrations in groundwater in several nations present a health risk to millions globally (Vithanage and Bhattacharya, 2015). The quality of drinking water is essential for public health and overall well-being. The ideal concentration of fluoride in drinking water is approximately 1.0 mg l^{-1}, which supports oral health and bone development. Excessive fluoride intake exceeding 1.5 mg l^{-1} (WHO, 2006) may lead to dental and skeletal fluorosis in individuals. Over 200 million individuals globally are expected to consume water containing fluoride levels exceeding 1.5 mg l^{-1}, which is the threshold recommended by the World Health Organization (WHO, 2021). Groundwater in many Indian states, including Andhra Pradesh, Haryana, Karnataka, Maharashtra, Rajasthan, Tamil Nadu, and West Bengal, have elevated fluoride levels (Amalraj and Pius, 2013; Ayoob and Gupta, 2006; Meenakshi and Maheshwari, 2006).

Agro-based products are promising, cost-effective adsorbents for fluoride removal, including Kaith leaves, Feronia limonia, coconut husk and shell charcoal, neem and mango derivatives, rice husk, black mustard husk ash, fruit peels (*Manilkara zapota, Solanum tuberosum*), *Phyllanthus emblica, Strychnos potatorum, Moringa species, Azadirachta indica* leaves, iron-infused *Pisum sativum* peel, *Senna auriculata* petals, *Ficus glomerata* bark, *Tulsi, karanji,* citron peel, and Parijaat (Lal *et al.,* 2022; Chukka *et al.,* 2022; Kumar and Maurya, 2022; Jadhav and Jadhav, 2022; Kavisri *et al.,* 2022). Current methods for reducing fluoride in drinking water—such as chemical precipitation, coagulation, ion exchange, electrocoagulation, nanofiltration, catalytic ozonation, and electrochemical oxidation are limited by high operational costs, maintenance, and waste generation. Adsorption is preferred in rural areas due to its cost-effectiveness, simplicity, high efficiency, environmental friendliness, minimal skill and electricity requirements, and potential for adsorbent reuse (Mohapatra *et al.,* 2009; Viswanathan *et al.,* 2010; WHO, 2010). In view of the above, an efficient fluoride removal method that can meet regulatory standards are highly sought (Solanki *et al.,* 2022). Balancing maintenance needs, availability of skilled personnel, and operational simplicity without compromising efficiency is essential. This study aimed to develop a cost-effective, agro-based adsorbent for fluoride removal from drinking water via adsorption.

Materials and Methods

Production of sugarcane bagasse (SB) biochar and chemically functionalized sugarcane bagasse (FSB) biochar: The FSB was stored in an airtight container for further analysis. Sugarcane bagasse procured from a local market was cut, washed, oven-dried at 105°C for 24 hr, and pyrolyzed at 500°C for 2 hr to obtain biochar (Jateen *et al.,* 2023). SB was then functionalized with 1% KCl (1:3 w/v), pyrolyzed at 700°C for 60 min, rinsed, and oven-dried at 120°C overnight. The resulting functionalized biochar (FSB) was stored in an airtight container for further use (Fig. 1).

Fluoride ions analysis method: A stock solution of fluoride (100 mg l^{-1}) was prepared and subsequently diluted as per experimental requirement. The fluoride analysis was conducted *in situ* utilizing a bench-top fluoride ion electrode (Horiba, Japan) with a resolution range of 0.1-1000 mg l^{-1} F^-.

Physical and chemical characteristics of SB and FSB

Determination of pH: A 5.0 g of FSB and SB biochar samples were mixed with deionized water and heated at 90°C for 30 min. The suspensions were allowed to cool at room temperature and pH was measured using a pH meter (Hanna- Digital pH meter, range: 0-14 pH).

Bulk density: A 25 ml glass cylinder was filled with 40 µm FSB and SB biochar (oven-dried at 80°C overnight) in triplicate, tapped to compact, and bulk density was calculated as per Senewirathna *et al.* (2022).

$$\text{Bulk density} = \frac{\text{Weight of dry material (g)}}{\text{Volume of packed dry material (ml)}} \times 100$$

Functional group analysis: Functional groups were analyzed by Fourier Transform Infrared spectroscopy (FTIR) (4000–400 cm^{-1}; FTIR-2000, Perkin Elmer) using potassium bromide (KBr) pellets prepared with a Perkin-Elmer hydraulic pump. Elemental composition was determined by Energy Dispersive X-ray Spectroscopy (EDX), which identifies elements and their relative atomic percentages based on characteristic X-ray spectra.

Proximate analysis of FSB and SB biochar: The proximate analysis of FSB and SB biochar was estimated by measuring the moisture content, volatile matter, ash content, and fixed carbon following the standard methods of APHA (2022).

Elemental analysis of FSB and SB biochar: Carbon, hydrogen, nitrogen, and sulfur contents (in %) were estimated with a CHNS analyzer (Elementar Vario MICRO, India) with helium as a carrier gas and oxygen as a combustion gas and Thermal conductivity detector (TCD). The operation was conducted under following conditions combustion tube 1150°C, reduction tube 850°C, TCD 59–60°C, helium flow 200 ± 10 ml min^{-1}, oxygen flow 10 ± 2 ml min^{-1} (non-combustion) and 30 ± 2 ml min^{-1} (combustion), at 1200 ± 50 mbar.

Iodine number: Iodine number was estimated by the standard method of ASTM (D4607-94). A 0.3 g powdered carbon was treated with 5% HCl, followed by 0.10 N iodine solution, agitated for 20 min, and filtered through a Whatman No. 1. A 30 ml aliquot was titrated with 0.1 M $Na_2S_2O_3$ using starch as an indicator, with a blank prepared without carbon. Iodine removal percentage was calculated.

Batch adsorption study: Batch adsorption experiments using FSB were conducted with NaF-spiked solutions (5–40 mg l^{-1}) prepared from a 100 mg l^{-1} standard. Mixtures were agitated in a thermostat shaker (ROTEK LSV, India) (25 ± 1°C, 120 rpm) for 60 min, allowed to settle for 2 min, and filtered through Whatman No. 42 paper. Residual fluoride in a 5 ml filtrate was measured using a fluoride ion electrode (Horiba, Japan).

Fig. 1: Chemically functionalized biochar.

Adsorption isotherms and kinetics: Adsorption isotherms elucidate adsorbate–adsorbent interactions and maximum adsorption capacity. Equilibrium data were evaluated using Langmuir (monolayer adsorption on uniform surfaces) (Langmuir, 1916) and Freundlich (multilayer adsorption on heterogeneous surfaces) models (Freundlich, 1906), with linear plots used to calculate isotherm constants (Sivarajasekar *et al.,* 2017). Adsorption kinetics, essential for assessing efficiency, was analyzed using pseudo-first-order and pseudo-second-order models (Waghmare *et al.,* 2015).

Removal efficiency and adsorption capacity: The fluoride removal efficiency after adsorption and uptake capacity of adsorbent at any time (t) was estimated by the following formula:

$$\text{Removal efficiency (\%)} = [(C_o - C_i)/Co] \times 100$$

$$\text{Adsorption capacity} = \frac{[(C_o - C_i)V]}{M}$$

Where, C_o the is initial fluoride concentration (mg l^{-1}), C_i is the residual fluoride concentration at time t, M is the mass of the adsorbent (g) and V (l) is the volume of the solution used in the batch study.

Fabrication of adsorbent coated Plaster of Paris pellets: Pellets were prepared by mixing bagasse filaments (2–4 mm) and Plaster of Paris (10:90 w/w), molding, air-drying, and oven-drying at 105 °C for 12 h. For coating, 1 g chitosan and 1 g KCl were dissolved in 100 ml of 1% acetic acid, filtered, and used to immerse pellets twice with air-drying in between. The pellets prepared by the above procedure were stored in a desiccator (the actual view of the pellets before and after coating (Fig. 2a,b). For coating, 1 g chitosan (≤75% acetylation) and 1 g KCl were dissolved in 100 ml of 1% acetic acid under constant stirring (450 rpm, 30 min), filtered through a 0.1 mm nylon sieve to remove coagulates, and the clear suspension was used for pellet coating. Pellets were immersed in the coating suspension for 30 sec, air-

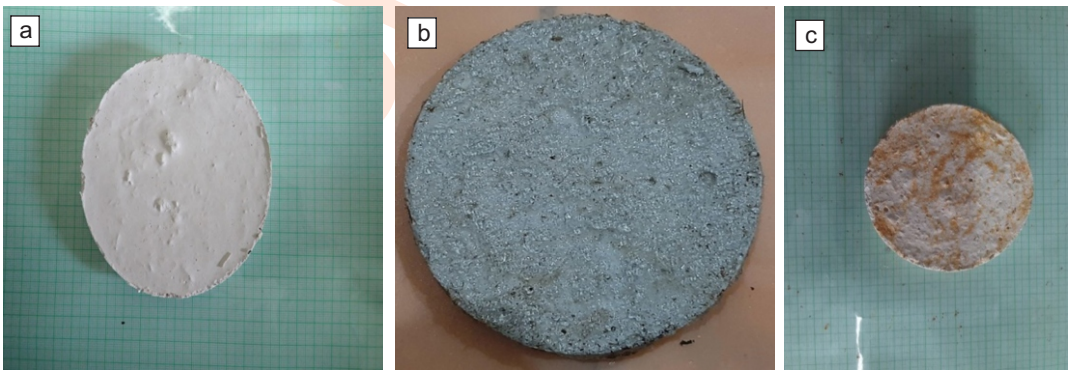

Fig. 2: (a) Pellet before coating, (b) Pellet after coating and (c) Coated pellet after drying.

dried for 20 min, re-immersed for a thicker layer, and oven-dried at 105°C overnight to constant weight (Fig 2c). They were then sprayed with 1% NaOH, dried, and weighed to calculate coating load. Screening showed this formulation achieved superior fluoride removal compared to other variants.

Thomas model: Thomas kinetic model, commonly applied to fixed-bed columns, estimates the maximum solid-phase solute concentration and adsorption rate constant for continuous adsorption processes (Chen *et al.,* 2011).

$$ln\frac{C_t}{C_0} = k_{AB}\, C_0\, t - k_{AB}\, N_0 \frac{Z}{F}$$

Regeneration of spent coating: At breakthrough, the exhausted bio-adsorbent coating was regenerated by applying a composite mixture of chitosan, potassium chloride and glacial acetic acid. The recoating procedure was conducted at each exhaustion (breakthrough) point for a maximum of five cycles. The average removal efficiency (%) was employed to evaluate the performance of the regenerated adsorbent during each operational cycle.

$$\text{Removal efficiency (\%)} = [(C_0\text{-}C_1) / C_0] \times 100$$

Results and Discussion

The prepared biochar exhibited a dark, granular, porous, and amorphous carbonaceous appearance. The percentage of fixed carbon was 73.26% for FSBB and 65.61% for SBB (Table 1). The higher fixed carbon percentage signifies the adsorbent's quality, enhancing surface area and adsorption efficiency. These findings are consistent with Boer et al. (2021), who found that a high carbon content of 68.50-73.01% was obtained at 400°C and 500°C. Another investigation of locally produced activated carbon found 4.0% moisture, 36.0% ash, 42.2% fixed carbon, and 16.8% volatile compounds (Nure *et al.,* 2017). The moisture content 2.45 % of FSBB was determined lower than SBB 3.74%, indicating high adsorbent attributes. In the current investigation, the volatile matter of FSB and SB biochar was 14.07% and 17.94%, while the ash content was only 10.22% and 12.71%, indicating that the inorganic component was minimal. Thermal degradation of cellulose and lignin at 400–500°C reduces volatile matter while increasing the carbon and ash content; bagasse charcoal showed 24.31–25.80% volatiles at 400 °C and 13.01–16.43% at 500°C, confirming the decline with higher temperatures (Boer *et al.,* 2021). Moderate ash concentration often enhances the adsorption of organic molecules from aqueous solutions due to hydrophobic properties of the material (Adib *et al.,* 2018). High ash content in raw materials hinder activated carbon development by lowering carbon yield and adsorption efficiency, making the production of low-ash adsorbents a key challenge in adsorption-based water and wastewater treatment. In this study, the bulk density of FSBB was 0.295 g ml^{-1} and that of SBB was 0.272 g ml^{-1}, both close to the reported range. Yu *et al.* (2019) found that sugarcane bagasse biochar had a much lower bulk density of 0.11 g ml^{-1}, while Kakom *et al.* (2023) observed a decrease in the bulk density from 0.163 to 0.086 g ml^{-1} as pyrolysis temperature increased from 300 to 700°C. Since high bulk density is generally considered advantageous for the adsorbents, the values obtained for FSB indicate favorable material properties. Both FSB and SB biochars also exhibited an alkaline pH. Table 2 displays the elemental composition of FSB and SB biochar based on the analysis.

FTIR was employed to examine the alterations in the functional groups of sugarcane biochar prior to and following treatment with KCl, as well as subsequent fluoride adsorption (Fig. 3), with a comparative analysis of three spectra available in Table 3. The FTIR spectra indicated the presence of O-H (hydroxyl) and C=C (alkene) groups prior to and following adsorption. The analysis indicated that the original SBB displayed characteristic peaks in alignment with prior studies (Fonsêca *et al.,* 2022). The untreated biochar exhibited peaks at 3685, 3592, 1593, and 1492 cm^{-1}, which are associated with O-H and C=C functional groups, respectively. Significant shifts in the peaks were observed in the spectra of the treated and fluoride-adsorbed biochar samples, indicating alterations in the chemical structure of the biochar. FTIR analysis showed a C=O peak at 1677 cm^{-1} in untreated biochar, absent in KCl-treated (FSB) and fluoride-adsorbed samples. A KCl peak at ~1230 cm^{-1} confirmed

Table 1: Characterization of chemically functionalized biochar and biochar

Samples	Moisture(%)	Ash (%)	Volatile matter (%)	Fixed carbon (%)	Bulk density (g ml^{-1})	pH value
Chemically functionalized biochar (FSB)	2.45±0.04	10.22±0.24	14.07±0.23	73.26±0.16	0.295±0.01	8.01±0.01
SB biochar	3.74±0.06	12.71±0.16	17.94±0.21	65.61±0.20	0.272±0.01	8.3±0.09

Table 2: Ultimate analysis of chemically functionalized biochar (FSB) and SB biochar

Samples	C (%)	H (%)	N (%)	S (%)	O (%)
Chemically functionalized biochar (FSB)	69.32±0.07	1.06±0.07	1.02±0.04	0.12±0.04	28.48±0.32
SB biochar	66.19±0.48	1.41±0.04	1.07±0.06	0.16±0.02	31.17±0.44

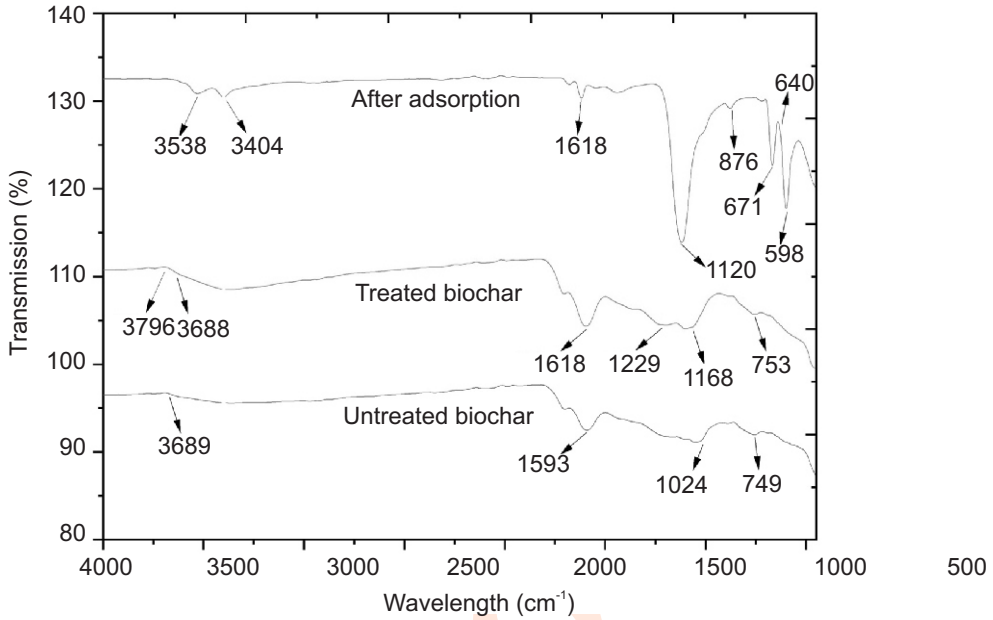

Fig. 3: FT-IR spectroscopy of untreated, treated biochar and after adsorption of fluoride.

Table 3: Different functional groups in untreated, treated biochar and after adsorption

Functional groups	References	Wavelength (cm^{-1})		
		Untreated biochar	Treated biochar	After absorption
O – H stretching	3690 - 3100	3689	3769	3528
		3592	3688	3404
C=O	1650 - 1800	1677	-	-
C=C	1500 - 1600	1593	1599	1618
		1497	-	-
KCl related peak	1230	-	1229	-
	1000 - 1300	1198	1168	1120
C-O, C-OH,C-O-C,C=C, C-C-O		1106	1104	-
		1061	-	-
		1051	-	-
O-H	600 - 900	749	753	903
		-	-	750
		-	-	701
		-	-	667
		-	-	640

successful modification, while shifts in the 1000–1300 cm^{-1} region after fluoride adsorption indicated interaction with lignin, cellulose, and hemicellulose functional groups. FTIR analysis (600–900 cm^{-1}) revealed new O–H peaks in fluoride-adsorbed biochar, absent in untreated and KCl-treated samples, indicating fluoride interaction. These results, consistent with the reports of Dehghani *et al.* (2018), highlight the impact of KCl modification and fluoride adsorption on biochar functional groups, relevant for environmental remediation. EDX analysis confirmed Fe ion precipitation on the novel adsorbent. Carbon and oxygen were present before and after fluoride adsorption, with notable changes, including a decrease in the oxygen concentration following adsorption (Tables 4,5). The EDX images showed that the Fe signal strength increased during adsorption (Fig. 4b). This indicates that fluoride ions may displace oxygen atoms (OH^-) on the adsorbent surface. The presence of Ca, Al, and Fe is essential for fluoride removal from water because they have a high propensity for interacting with fluoride to produce insoluble compounds (Alwash, 2017; Waghmare and Arfin, 2015). Fluoride removal occurs via precipitation or adsorption: Ca^{2+} forms

Table 4: Composition and weight of different elements before adsorption

Elements	Weight (%)	MDL	Atomic (%)	Net Int	R	A	F
C K	55.9	0.90	66.2	228.6	0.9284	0.0906	1.0000
O K	32.6	0.42	29.0	276.8	0.9371	0.0736	1.0000
Na K	1.4	0.14	0.9	48.6	0.9468	0.2834	1.0025
Mg K	0.5	0.09	0.3	30.9	0.9497	0.4251	1.0041
Al K	0.2	0.08	0.1	14.9	0.9524	0.5658	1.0070
Cl K	5.8	0.09	2.3	409.4	0.9619	0.8914	1.0172
K K	0.9	0.10	0.3	47.9	0.9661	0.9171	1.0306
Ca K	2.6	0.12	0.9	123.0	0.9680	0.9357	1.0210

Table 5: Composition and weight of different elements after adsorption

Elements	Weight (%)	MDL	Atomic (%)	Net Int	R	A	F
C K	25.8	1.46	37.5	79.8	0.9101	0.0662	1.0000
O K	26.5	0.35	29.0	279.6	0.9203	0.0881	1.0000
Fe K	20.5	0.23	18.8	299.4	0.9245	0.0979	1.0000
Na K	6.0	0.15	4.6	177.4	0.9319	0.2319	1.0025
Mg K	1.5	0.10	1.1	74.2	0.9355	0.3350	1.0040
Si K	0.3	0.08	0.2	25.2	0.9419	0.5920	1.0114
S K	1.3	0.08	0.7	101.2	0.9477	0.7827	1.0268
Cl K	5.2	0.09	2.6	359.0	0.9503	0.8339	1.0264
K K	2.2	0.10	1.0	127.3	0.9554	0.8876	1.0490
Ca K	10.7	0.12	4.7	502.3	0.9578	0.9072	1.0148

insoluble CaF_2, Al^{3+} generates AlF_3, and Fe ions adsorb fluoride to form FeF_3. EDX analysis (Table 4, Fig. 4a) confirmed the presence of Ca, Al, Fe, and Mg in the novel adsorbent, indicating its high affinity for fluoride and effective removal capability (Waghmare and Arfin, 2015; Wang *et al.,* 2015). Sugarcane bagasse biochar produced at 500°C exhibited an iodine value of 261.34 ± 24.22 mg g^{-1}, increasing with pyrolysis temperature, indicating a highly porous and effective adsorbent structure (Loc *et al.,* 2023).

In batch experiments, FSB achieved 76.8% fluoride removal with a capacity of 3.86 mg g^{-1} at 5 mg l^{-1} fluoride, pH 5, 150 mg 100 ml^{-1} adsorbent, 60 min contact, and 120 rpm agitation. Consistent with these results, Gourai et al. (2023) reported ≥80% removal using *M. oleifera* biochar, while Rahman *et al.* (2022) observed 99% removal with Bajra husk biochar at pH 2. Further, low pH enhances adsorption by increasing active site selectivity, whereas alkaline conditions reduce fluoride sorption, as observed in corncob (Hettithanthri *et al.,* 2023) and Dodonaea bark biochars (Aziz *et al.,* 2022), rice straw biochar (Yan *et al.,* 2022). Adsorption isotherms describe the equilibrium between solute in the liquid phase and adsorbed solute on the adsorbent at constant temperature, with Langmuir and Freundlich models commonly used to characterize adsorption behavior. For Langmuir isotherm, a plot of $1/C_e$ versus $1/q_e$ was used to determine b and Q_o (Table 6). The high R^2 value indicated good model fit, suggesting homogeneous adsorption on the adsorbent surface. Freundlich model describes adsorption on heterogeneous surfaces. Constants 1/n and Kf were obtained from the slope and intercept of log q_e versus log C_e (Table 6). The strength of adsorption, or affinity of 1/n, is indicated by the constant n in the Freundlich model. During this process, the calculated value of n (0.5555) is less than 1, indicating that biosorption is a chemical process (Sivasankar *et al.*, 2012). Kinetic data were analyzed using pseudo-first- and pseudo-second-order models (Ho, 2006). The pseudo-second-order model provided a better fit (R^2 = 0.9967) with an equilibrium adsorption capacity of 6.10 mg g^{-1} at 5 mg l^{-1} fluoride, closely matching the experimental data (Table 7). This suggests that fluoride adsorption on FSB is mainly driven by chemical adsorption (Bakhtiari and Azizian, 2015).

Column experiments were conducted using spiked fluoride water to evaluate the effect of influent flow rate on FSB adsorption capacity and breakthrough behavior. Flow rates of 100, 150 and 200 ml min^{-1} were tested at a constant fluoride concentration of 30 mg l^{-1} and a bed height of 30 cm. As shown in Fig. 5, the higher flow rates shortened both breakthrough and exhaustion times because the fluoride ions had less contact time with the adsorbent. Lower flow rates extended breakthrough time, saturation time, and treated volume due to prolonged interaction with the adsorbent pores. These results corroborate with the findings of Hiremath and Theodore (2017), who noted that slower flow enhances adsorption by improving access to biosorption sites, which gradually become occupied, reducing efficiency.

Overall, increasing influent fluoride concentration and

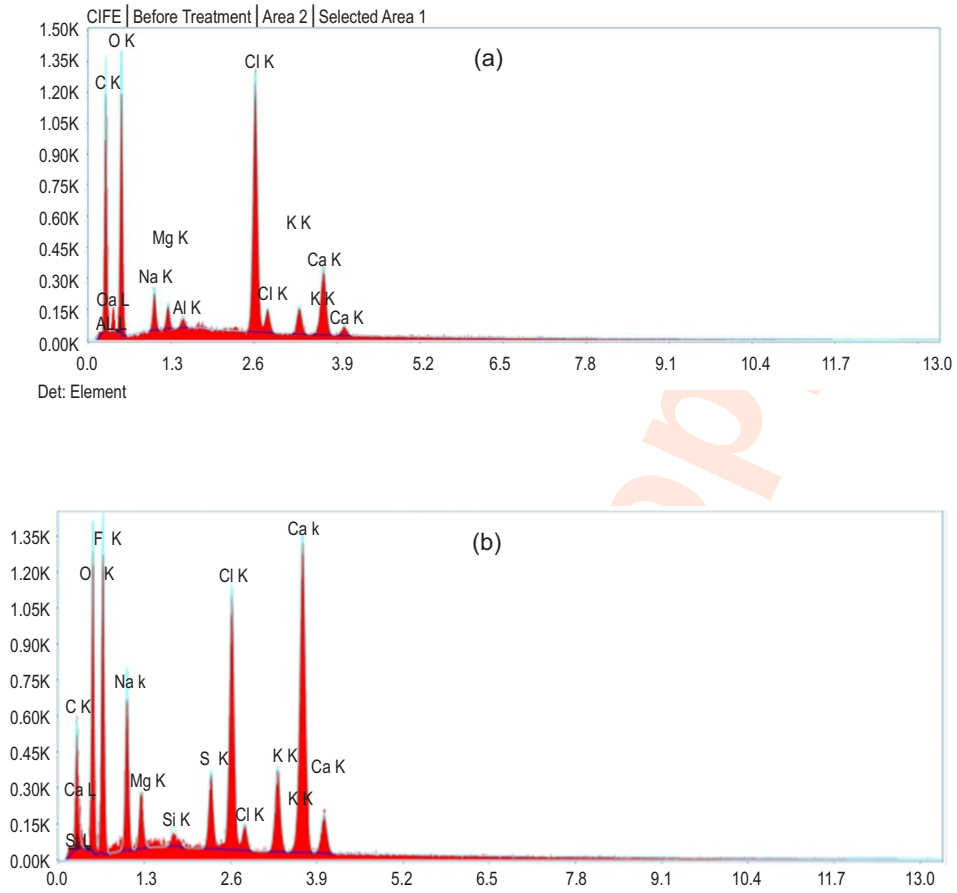

Fig. 4: (a) EDX spectrum before fluoride adsorption and (b) EDX spectrum after fluoride adsorption.

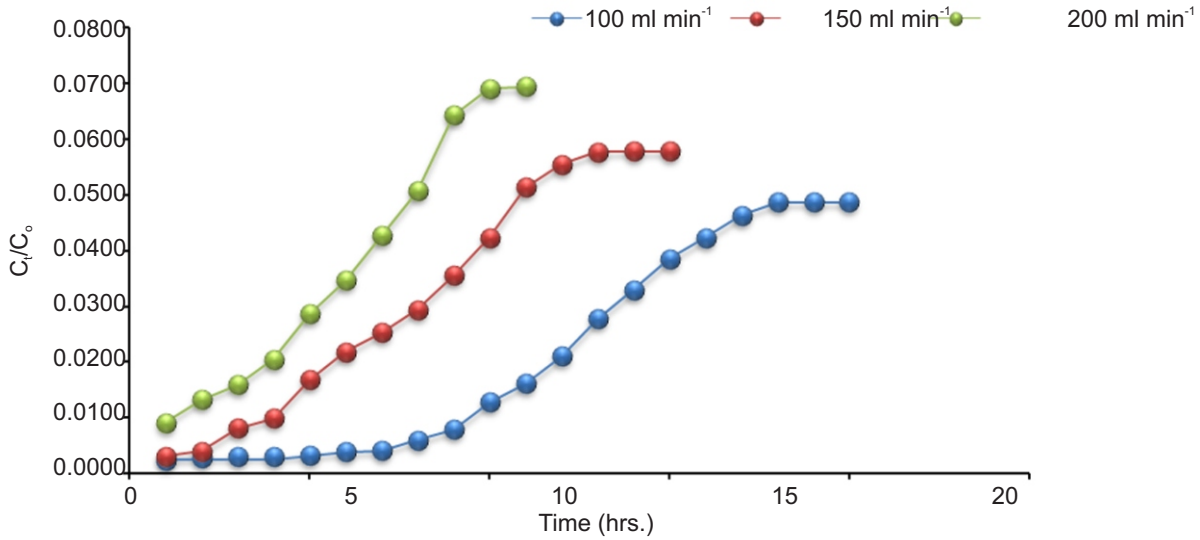

Fig. 5: Effect of bed on breakthrough time at different flow rate (BD=30 cm. and C0=30 mg l^{-1}).

Table 6: Langmuir and Freundlich isotherm

Isotherms	Parameters	Values
Langmuir	Q_o (mg g^{-1})	13.1492
	b (L g^{-1})	0.4217
	R_L	0.5258
	R^2	0.9883
Freundlich	K_F (mg g^{-1}) (l mg^{-1})$^{1/n}$	2.2485
	1/n	0.5555
	n	1.8001
	R^2	0.9919

Table 7: Pseudo-first-order and Pseudo-second-order kinetic model

Kinetic models	Parameters	Values
Pseudo-first-order kinetic model	k_1(1 min^{-1})	0.0043
	q_e (mg g^{-1})	5.16
	R^2	0.6904
Pseudo-second-order kinetic model	k_2(1 min^{-1})	0.2296
	q_e (mg g^{-1})	6.10
	R^2	0.9967

Table 8: Linearized Thomas model parameters at 7.5% breakthrough

BD (cm), C_0 (mg l^{-1}) and Q (ml min^{-1})	K_{TH} (l mg^{-1}. min.)	q_0 (mg g^{-1})	R^2
[10,30,100]	0.0215	4.65	0.8683
[20,30,100]	0.0223	4.94	0.9101
[30,30,100]	0.0157	6.43	0.9242
[30,25,100]	0.0206	6.00	0.9645
[30,20,100]	0.0168	6.16	0.9696
[30,30,200]	0.0209	4.62	0.9470

flow rate decreased breakthrough and exhaustion durations, while adsorption capacity declined at higher flow rates. Breakthrough curves were evaluated at bed depths of 10, 20 and 30 cm, with a constant flow rate of 100 ml min^{-1} and initial fluoride concentration of 30 mg l^{-1}. Increasing the bed depth from 10 to 30 cm extended both the saturation time and the volume of treated water, from 11 hr and 112 l at 10 cm to 21 hr and 165.12 l at 30 cm. This indicates that higher bed heights enhance breakthrough and exhaustion times due to the increased availability of sorption sites and an expanded mass transfer zone (Fig. 6). Shallower beds produced steeper breakthrough curves and shorter breakthrough times, as limited binding sites and reduced diffusion time restricted fluoride adsorption. These findings align with the previous studies showing that larger bed heights prolong breakthrough and exhaustion phases (Hiremath and Theodore, 2017). Similarly, Abu Bakar *et al.* (2019) observed that Quaternized Palm Kernel Shell had larger pores than Palm Kernel Shell Activated Carbon, and Liu *et al.* (2022) reported comparable results using Al-impregnated granular activated carbon. The effect of applied voltage on fluoride removal was evaluated at 0, 200 and 220 V. Increasing the voltage improved the removal efficiency, with 220 V achieving the highest fluoride removal of 99.75%, which reveals that the applied electric current appeared to activate the column, enhancing adsorption and desorption processes (Shivayogimath and Punage, 2014).

Thomas model, widely used for fixed-bed column adsorption, was applied to calculate the rate constant KTH) and maximum solid-phase concentration (q_o) from column data via linear regression (Eq. 9, Table 8). Coefficients of determination (R^2) ranged from 0.8683 to 0.9696. Increasing influent concentration or flow rate decreased q_o but increased K_{TH}, while higher bed heights increased q_o and decreased K_{TH}. These results indicate that fluoride adsorption is driven by the concentration gradient, and adsorption efficiency improves with lower flow rates, higher influent concentration, and greater bed height (Aksu and Gonen, 2004).

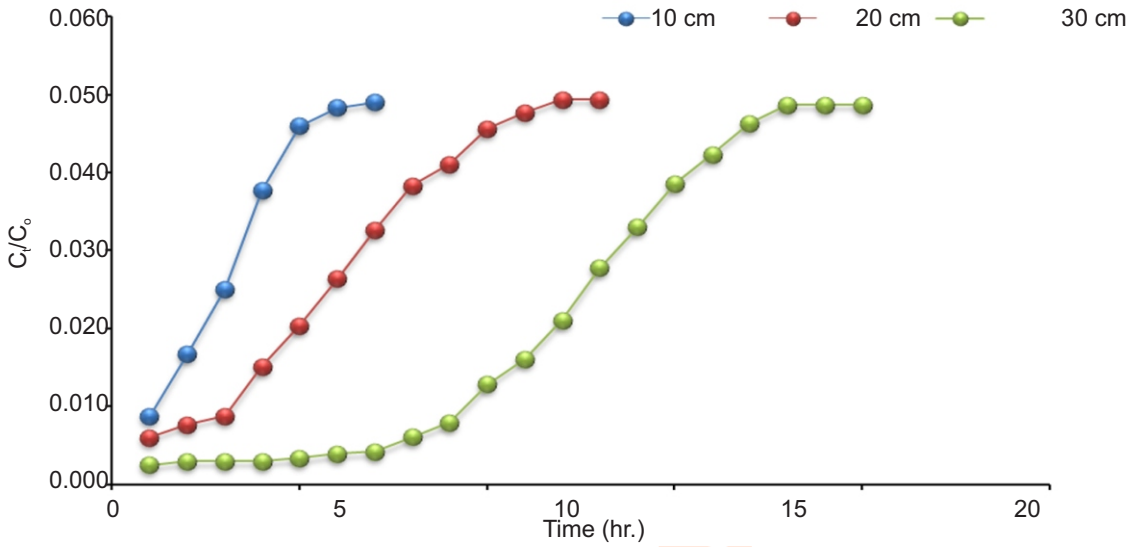

Fig. 6: Effect of bed on breakthrough time at a different bed depth (Q=100 ml min^{-1} and C0=30 mg l^{-1}).

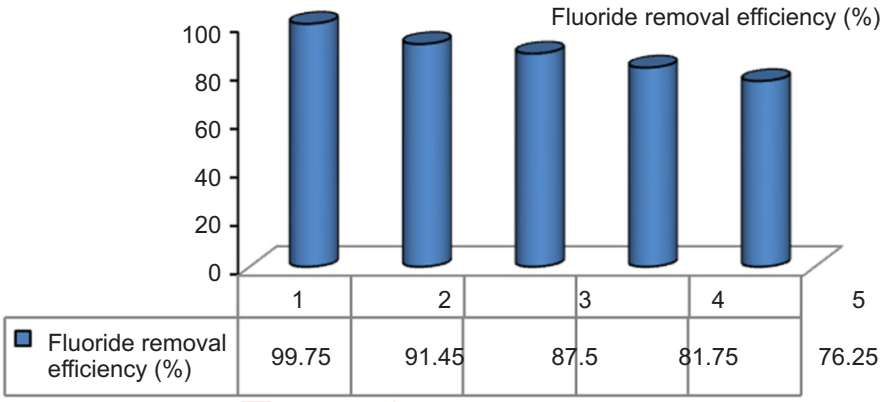

Fig. 7: Fluoride removal efficiency during regeneration.

The fluoride adsorption performance of pellets and FSB was evaluated over five regeneration cycles and compared with the initial adsorption (Fig. 7). Initial fluoride removal was 99.75%, decreasing to 76.25% after five cycles, likely due to chemisorption of residual fluoride and gradual adsorbent depletion (Zhang *et al.,* 2019). These results suggest that regeneration can reduce treatment costs while maintaining reasonable adsorbent efficiency. This study demonstrated that a column bed composed of biosorbent-coated pellets and chemically functionalized biochar effectively removes fluoride. In continuous-flow experiments using 30 mg l^{-1} fluoride at 100 ml min^{-1}, removal efficiency reached 99.75%. Fluoride removal and adsorption capacity increased with concentration, with early column saturation observed. The adsorbent maintained its efficiency over five treatment cycles, highlighting that the pelletized and functionalized biochar column bed provides a cost-effective solution for fluoride removal from water.

Acknowledgments

The authors express heartfelt thanks to the Director and Vice-Chancellor, ICAR-Central Institute of Fisheries Education, Mumbai, Vice-Chancellor, MAFSU, Nagpur, and the Head AEHM Division for providing necessary facilities to conduct the research work.

Authors' contribution: M.M. Girkar: Writing – original draft; **S.P. Shukla:** Investigation, Conceptualization. **S. Kumar:**

Methodology, Investigation. **V.S. Bharti, K. Kumar, G.R. Bhuvaneshwari:** Supervision, Conceptualization. **S.S. Gangan, S.W. Belsare, S.N. Kunjir:** Revision and editing.

Funding: The work did not receive any funds.

Research content: The research content of manuscript is original and has not been published elsewhere.

Ethical approval: Not applicable.

Conflict of interest: The authors declare no conflict of interest.

Data availability: Data will be made available from the Corresponding author upon reasonable request.

Consent to publish: All authors agree to publish the paper in *Journal of Environmental Biology.*

References

Abu Bakar, A.H., L.C. Abdullah, N.A. Mohd Zahri and M.A. Alkhatib: Column efficiency of fluoride removal using quaternized palm kernel shell (QPKS). *Int. J. Chem. Engin.,* **3**, 1-13 (2019).

Adib, M.R.M., M.H.M.N. Attahirah and A.R.M. Amirza: Phosphoric acid activation of sugarcane bagasse for removal of o-toluidine and benzidine. In: IOP Conference Series: *Earth Environ. Sci.,* **140**, 012029 (2018).

Aksu, Z and F. Gönen: Biosorption of phenol by immobilized activated sludge on a continuous packed bed: Prediction of breakthrough curves. *Proce. Biochem.,* **39**, 599-613 (2004).

Alhendal, M., M. J. Nasir, K. S. Hashim, J. Amoako-Attah, D. Al-Faluji, M. Muradov and B. Abdulhadi: Cost-effective hybrid filter for remediation of water from fluoride. In: IOP Conference Series: Mater. *Sci. Engin.,* **888**, 012038 (2020).

Amalraj, A. and A. Pius: Health risk from fluoride exposure of a population in selected areas of Tamil Nadu South India. *Food Sci. Human Welln.,* **2**, 75-86 (2013).

APHA: Standard methods for the examination of water and wastewater. 24th Edn., 1516 pages (2022).

ASTM, D4607-94 (Reapproved 2006): Standard method for the determination of iodine number of activated carbons. 1-9.

Ayoob, S. and A. K. Gupta: Fluoride in drinking water: a review on the status and stress effects. *Critical Revi. Env. Sci. Tech.,* **36**, 433-487 (2006).

Aziz, F., I. Din, M. Amin, MI. Khan, F. Khan and M. Khurshid: Fluoride removal from water by a novel *Dodonaea viscosa* bark biochar adsorbent. *Fluoride,* **55**, 165-170 (2022).

Bakhtiari, N and S. Azizian: Adsorption of copper ion from aqueous solution by nanoporous MOF-5: a kinetic and equilibrium study. *J. Mole. Liqu.,* **206**, 114–118 (2015).

Boer, F.D., J. Valette, J.M., Commandré, M. Fournier and M.F. Thévenon: Slow pyrolysis of sugarcane bagasse for the production of char and the potential of its by-product for wood protection. *J. Renew. Mater.,* **9**, 97-117 (2021).

Chamanehpour, E., M. HosseinSayadi and E. Yousefi: The potential evaluation of groundwater pollution based on the intrinsic and the specific vulnerability index. *Groundwater Sustain. Develop.,* **10**, 100313 (2020).

Chen, N., Z. Zhang, C. Feng, M. Li, R. Chen and N. Sugiura: Investigations on the batch and fixed-bed column performance of fluoride adsorption by Kanuma mud. *Desalination,* **268**, 76-82 (2011).

Chukka, N.D.K.R., P. GomathiNagajothi, L. Natrayan, Y.B.S. Reddy, D. Veeman, P.P. Patil and S. Thanappan: Investigation on efficient removal of fluoride from ground water using activated carbon adsorbents. *Adsorpt. Sci. Tech.,* **1**, 1-9 (2022).

Dehghani, M. H., M. Farhang, M. Alimohammadi, M. Afsharnia and G. Mckay: Adsorptive removal of fluoride from water by activated carbon derived from $CaCl_2$-modified *Crocus sativus* leaves: Equilibrium adsorption isotherms, optimization, and influence of anions. *Chem. Engin. Communicat.,* **205**, 955-965 (2018).

Derakhshani, R., A. Raoof, A.H. Mahvi and H. Chatrouz: Similarities in the fingerprints of coal mining activities, high ground water fluoride, and dental fluorosis in Zarand district, Kerman province, Iran. *Fluoride,* **53**, 257-267 (2020).

Fito, J., N. Tefera, S. Demeku and H. Kloos: Water footprint as an emerging environmental tool for assessing sustainable water use of the bioethanol distillery at Metahara sugarcane farm, Oromiya Region, Ethiopia. *Water Conser. Sci. Engin.,* **2**, 165-176 (2017).

Fito, J. and K. Alemu: Microalgae–bacteria consortium treatment technology for municipal wastewater management. *Nanotech. Environ. Engine.,* **4**, 1-9 (2019).

Fonsêca, M.C., C. A.M. Júnior, D. dos Santos Dias, J.P. Da Silva, R.S. Lamarca, C.A. Ribeiro and P.C.F. de Lima Gomes: Sugarcane bagasse biochar pellets for removal of caffeine, norfloxacin, and ciprofloxacin in aqueous samples. *Eclética Química,* **47**, 82-96 (2022).

Freundlich, H.M.: Over the adsorption in solution. *J. Physical Chemi. A.,* **57**, 385-470 (1906).

Gourai, M., A.K. Nayak, P.S. Nial, B. Satpathy, R. Bhuyan, S.K. Singh and U. Subudhi: Thermal plasma processing of *Moringa oleifera* biochars: adsorbents for fluoride removal from water. *RSC Advan.,* **13**, 4340-4350 (2023).

Hettithanthri, O., A.U. Rajapaksha, N. Nanayakkara and M. Vithanage: Temperature influence on layered double hydroxide tailored corncob biochar and its application for fluoride removal in aqueous media. *Environ. Pollut.,* **1**, 121054. (2023).

Hiremath, P.G. and T. Theodore: Biosorption of fluoride from synthetic and ground water using *Chlorella vulgaris* immobilized in calcium alginate beads in an up flow packed bed column. *Period. Polytech. Chem. Engine.,* **61**, 188-199 (2017).

Ho, Y.S.: Review of second-order models for adsorption systems. *J. Hazard. Materi.,* **3**, 681-689 (2006).

Jateen, S., V. S.Bharti, S. Prakash, S. Krishnan, T. Paul and S. Kumar: Sugarcane bagasse biochar-amended sediment improves growth, survival, and physiological profiles of white-leg shrimp, *Litopenaeus vannamei* (Boone, 1931) reared in inland saline water. *Aqua. Int.,* **31**, 2145-2164 (2023).

Jadhav, A.S. and M.V. Jadhav: Use of response surface methodology for optimization of fluoride removal efficiency by adsorption on black mustard husk ash. *Materials Today: Proceed.,* **61**, 150-157 (2022).

Kakom, S.M., N.M. Abdelmonem, I.M. Ismail and A.A. Refaat: Activated carbon from sugarcane bagasse pyrolysis for heavy metals adsorption. *Sugar Tech.,* **25**, 619-629 (2023).

Kavisri, M., M. Abraham, S. Karthick Raja Namasivayam, V.R. Raji, S. Sigamani and M. Moovendhan: Removal of fluoride from water by natural biosorbents and evaluation of microstructure and functional groups in removal process. *Biomass Conver. Biorefin.,* **14**, 1-7 (2022).

Kumar, A. and N.S. Maurya: A study of isotherms and kinetics of *Mangifera indica* bark adsorbent used for fluoride removal from

drinking water. *Engin. Tech. Appl. Sci. Res.,* **12**, 9233-9238 (2022).
Lal, M.S., J. Priyanka, S. Neetu and T. Paras: A study on removal of fluoride ions using Kaith plant leaves (*Feronia limonia*) as a low-cost natural adsorbent. *Res. J. Chem. Environ.,* **26**, 167-179 (2022).
Langmuir I.: The constitution and fundamental properties of solids and liquids. Part I. Solids. *J. American Chem. Soc.,* **38**, 2221–2295 (1916).
Liu, Z., S. Zheng and D. Zhang: Al-impregnated granular activated carbon for removal of fluoride from aqueous solution: Batch and fixed-bed column study. *Water,* **14**, 3554 (2022).
Loc, N.X., T.D. Thanh and D.T.M. Phuong: Physico-chemical properties of biochar produced from biodegradable domestic solid waste and sugarcane bagasse. *Int. J. Recy. Organ. Waste Agri.,* **12**, 395-407 (2023).
Meenakshi and R.C. Maheshwari: Fluoride in drinking water and its removal. *J. Hazard Mater.,* **137**, 456-463 (2006).
Mohapatra, M., S. Anand, B.K. Mishra, D.E. Giles and P. Singh: Review of fluoride removal from drinking water. *J. Envt. Manag.,* **91**, 67–77 (2009).
Nure, J.F., N.T. Shibeshi, S.L. Asfaw, W. Audenaert and S.W. Van Hulle: COD and colour removal from molasses spent wash using activated carbon produced from bagasse fly ash of Matahara sugar factory, Oromiya region, Ethiopia. *Water SA,* **43**, 470-479 (2017).
Patel, P., N.J. Raju, B.S.R. Reddy, U. Suresh, D.B. Sankar and T.V.K. Reddy: Heavy metal contamination in river water and sediments of the Swarnamukhi River Basin, India: risk assessment and environmental implications. *Environ. Geochem Healt.,* **40**, 609-623 (2018).
Rahman, M.A., S. Bar and L. Parwani: Removal of fluoride from drinking water to permissible levels with Bajra husk. *Materials Today: Proceedings,* **68**, 1158-1166 (2022).
Raj, D. and E. Shaji: Fluoride contamination in groundwater resources of Alleppey, southern India. *Geosci. Fronti.,* **8**, 117-124 (2017).
Raju, N.J., S. Dey, W. Gossel and P. Wycisk: Fluoride hazard and assessment of groundwater quality in the semi-arid Upper Panda River basin, Sonbhadra district, Uttar Pradesh, India. *Hydrolog. Sci. J.,* **57**, 1433-1452 (2012).
Rizzu, M., A. Tanda, C. Cappai, P.P. Roggero and G. Seddaiu: Impacts of soil and water fluoride contamination on the safety and productivity of food and feed crops: A systematic review. *Sci. Total Environ.,* **787**, 147650 (2021).
Senewirathna, D.S.G.D., S.Thuraisingam, S. Prabagar and J. Prabagar:. Fluoride removal in drinking water using activated carbon prepared from palmyrah (*Borassus flabellifer*) nut shells. *Curr. Res. Green Sustain. Chemist.,* **5**, 100304(2022).
Shivayogimath, C. B. and S. Punage: Optimization of parameters for fluoride removal by electrocoagulation using aluminum electrodes in monopolar parallel combination. *Int. J. Eng. Res.* , **3**, 1276-1280 (2014).
Singaraja C., S. Chidambaram, P. Anandhan, M.V. Prasanna, C. Thivya, R. Thilagavathi and J. Sarathidasan: Geochemical evaluation of fluoride contamination of groundwater in the Thoothukudi District of Tamilnadu, India. *Appli. Water Sci.,* **4**, 241-250 (2014).
Sivarajasekar, N., T. Paramasivan, S. Muthusaravanan, P. Muthukumaran and S. Sivamani: Defluoridation of water using adsorbents-a concise review. *J. Environ. Biotech. Res.,* **6**, 186–198 (2017).
Sivasankar, V., S. Rajkumar, S. Murugesh and A. Darchen: Influence of shaking or stirring dynamic methods in the defluoridation behavior of activated tamarind fruit shell carbon. *Chem. Eng. J.,* **197**, 162–172 (2012).
Solanki, Y.S., M. Agarwal, A.B. Gupta, S. Gupta and P. Shukla: Fluoride occurrences, health problems, detection and remediation methods for drinking water: A comprehensive review. *Sci. Total Environ.,* **807**, 150601 (2022).
Viswanathan G, Gopalakrishnan S, Siva and S. Ilango: Assessment of water contribution on total fluoride intake of various age groups of people in fluoride endemic and non-endemic areas of Dindigul District, Tamil Nadu, South India. *Water Res.,* **44**, 6186–6200 (2010).
Vithanage, M., P. Bhattacharya: Fluoride in drinking water: health effects and remediation. CO_2 sequest. *Biofuels Depollute*., **5**, 105-151 (2015).
Waghmare, S., T. Arfin, S. Rayalu, D. Lataye, S. Dubey and S. Tiwari: Adsorption behavior of modified zeolite as novel adsorbents for fluoride removal from drinking water: surface phenomena, kinetics and thermodynamics studies. *Int. J. Sci. Engine. Tech. Res.,* **12**, 4114-4124 (2015).
Waghmare, S.S. and T. Arfin: Fluoride removal from water by various techniques. *Int. J. Innov. Sci. Engine. Technol.,* **2**, 560–577 (2015).
Wang, J., D. Kang, X. Yu, M. Ge and Y. Chen: Synthesis and characterization of Mg–Fe–La trimetal composite as an adsorbent for fluoride removal. *Chem. Engine. J.,* **264**, 506-513 (2015).
WHO: Chemical fact sheets: fluoride, guidelines for drinking water quality (electronic resource). **Vol. 1**, 3rd Edn., incorporation. First Addendum, Recommendations, Geneva, pp. 375–377 (2006).
WHO: Guidelines for Drinking-Water Quality, First Addendum to 3rd Edn., World Health Organization: Geneva, Switzerland, 2006 (2021).
World Health Organization (WHO): Guidelines for drinking-water quality, Geneva, Switzerland, 3rd edn., **1**, 668 pages (2008).
Yan, L., W. Gu, N. Zhou, C. Ye and Y. Yang: Preparation and characterization of wheat straw biochar loaded with aluminium/ lanthanum hydroxides: a novel adsorbent for removing fluoride from drinking water. *Environ. Tech.,* **43**, 2771-2784 (2022).
Yu, P., Li Q, L. Huang, G. Niu and M. Gu: Mixed hardwood and sugarcane bagasse biochar as potting mix components for container tomato and basil seedling production. *Appl. Sci.,* **9**, 4713 (2019).
Zhang, Z., L. Yan, H. Yu, T. Yan and X. Li: Adsorption of phosphate from aqueous solution by vegetable biochar/layered double oxides: fast removal and mechanistic studies. *Biores. Tech.,* **284**, 65–71 (2019).